Biochimica et Biophysica Acta, 314 (1973) 390–402

BBA 46605

STUDIES ON THE MECHANISM OF DESTABILIZATION OF THE POSITIVE CHARGES TRAPPED IN THE PHOTOSYNTHETIC WATER-SPLITTING ENZYME SYSTEM Y BY A DEACTIVATION-ACCELERATING AGENT

G. RENGER

Max Volmer Institut für Physikalische Chemie und Molekularbiologie der Technischen Universität Berlin, Berlin (Germany)

(Received April 10th, 1973)

SUMMARY

The mechanism of the 2-(3,4,5-trichloro)anilino-3,5 dinitrothiophene (ANT 2S)-induced cyclic electron flow leading to the discharge of the higher-trapped-hole accumulation states S_2 and S_3 in the photosynthetic water-splitting enzyme system Y of chloroplasts has been investigated. It was found:

1. Under normal conditions the ANT 2s-catalyzed cycle includes both light reactions.

2. By selective kinetical inhibition of the electron flow through P700 —either by histone treatment or by 2,5-dibromo-3-methyl-6-isopropyl-1,4-benzoquinone blockage— the ANT 2s-induced deactivation of S_2 and S_3 is not significantly changed. Hence, System I activity is not a functional prerequisite for the ANT 2s-catalyzed discharge of S_2 and S_3.

3. The reciprocal half time of the ANT 2s-induced decay of the relative average oxygen yield per flash, as a function of the time t_d between the flashes representing the degree of the Acceleration of the Deactivatian Reactions of the water-splitting enzyme system (ADRY) effect, is nearly linearly related to the ANT 2s concentration within the range of 10^{-7}–10^{-6} M.

4. In respect to the mode of action of ANT 2s two different types of mechanism have been discussed: fixed-place mechanism and mobile-catalyst mechanism.

5. Based on the experimental data the conclusion has been drawn that the ADRY agent ANT 2s probably acts as a mobile catalyst.

INTRODUCTION

In the photosynthetic water-splitting enzyme system Y, water is oxidized to molecular oxygen by positive charges (holes) produced in Photosystem II. It has been found, that the Y systems are able to store holes until after the accumulation of 4 positive charges and the cooperative fast reaction with water takes place[1,2] within

Abbreviations: ADRY, Acceleration of the Deactivation Reactions of the water-splitting enzyme stystem Y; ANT 2s, 2-(3,4,5-trichloro)anilino-3,5-dinitrothiophene; DCMU, 3-(3,4-dichlorophenyl)-1,1-dimethylurea; DBMIB, 2,5-dibromo-3-methyl-6-isopropyl-1,4-benzoquinone.

1 ms[3,4]. The lifetime of the holes trapped in the Y system is dependent on the accumulation state. The trapped hole accumulation states S_2 and S_3, representing two and three trapped holes, respectively, are discharged in the dark within a few seconds[5–7], whereas the state S_1 (one trapped hole) is stable for a long time[1,2].

The stability of the states S_2 and S_3 can be modified by chemical effectors[8–13], the so called Acceleration of the Deactivation Reactions of the water-splitting enzyme System Y (ADRY) agents[10]. Comparative studies with different uncouplers and ionophores led to the conclusion that the light-induced electrochemical potential gradient across the thylakoid membrane does not significantly influence the stability of the trapped holes[11,12].

For the discharge of holes electrons are required. The possible action of the ADRY agents as irreversible electron donors can be excluded for stoichiometrical reasons[11].

Recently it has been found, that the ADRY agents induce an internal cyclic electron flow[14]. Hence, the question concerning the pathway of this cycle arises. Generally two possibilities can be considered (see Fig. 1): (1) The ADRY agent-induced cycle includes both light reactions, *i.e.* the electrons required for the discharge of the trapped holes are provided by the reducing side of System I (way C). (2) The ADRY agent-induced cyclic pathway includes only light reaction II (for example the plastoquinone pool could serve as an electron donor, way B).

Furthermore, it remains to be shown whether the ADRY agents act as diffusible catalysts (mobile catalyst model) or as effectors which are fixed at specific sites (fixed-place mechanism).

In the present paper an analysis of the ADRY effect is given on the basis of the results obtained for a typical and very potent ADRY agent, namely 2-(3,4,5-trichloro)-anilino-3,5-dinitrothiophene (ANT 2s). It is supposed that other ADRY agents (at least chemically related substances) act in the same manner as ANT 2s. In the following it will be shown, that no special electron source is required for the ADRY effect, *i.e.* under different experimental conditions the ANT 2s-induced cycle includes different parts of the electron transport chain. From the investigation of the dependence of the oxygen decay kinetics on the ANT 2s concentration, the conclusion has been drawn, that the ADRY agents probably act as mobile catalysts for the induced cyclic electron flow leading to the discharge of the trapped holes in the states S_2 and S_3.

MATERIALS AND METHODS

Preparation of chloroplasts

The chloroplasts were prepared from market spinach according to the method of Winget *et al.*[15], except that 10^{-2} M ascorbate was present during the grinding of the spinach. For the storage in liquid nitrogen, 5% dimethylsulfoxide was added. After thawing, the activity of the stored chloroplasts was nearly the same as for freshly prepared chloroplasts.

Reaction mixture

The reaction mixture contained chloroplasts ($5 \cdot 10^{-5}$ M chlorophyll), 10^{-4} M $K_3[Fe(CN)_6]$ *plus* 10^{-4} M $K_4[Fe(CN)_6]$ as electron acceptors, 10^{-2} M KCl, $2 \cdot 10^{-3}$ M $MgCl_2$ and 2.10^{-2} M morpholinoethanesulfonate–NaOH buffer, pH 6.5. The addition of the ADRY agents is given in the legends of the figures.

Measurements

The oxygen measurements were performed with a Clark-type electrode (IL 125 B Instrumentation Laboratory Inc., Watertown) by a repetitive technique as is described in ref. 10. For the details of the flash lamp device see ref. 16.

The absorption changes at 703 nm were measured with a repetitive flash spectroscopic technique similar to that published in ref. 17. Usually 256 signals were averaged in a Fabri-Tek 1062. The electrical bandwidth ranged from 0 to 5 kHz. The DC component arising from the large part of invariable absorption of the probe was eliminated by a suitable compensation. The optical path length was 1 mm, the bandwidth of the monitoring light ($\lambda = 703$ nm, intensity < 100 ergs·cm^{-2}·s^{-1}) was 5 nm. The exciting flashes were passed through a Schott filter BG 28, 4 mm with a flash duration of approx. 20 μs.

RESULTS AND DISCUSSION

The pathway of the ANT 2s-induced cyclic electron flow

The question about the participation of System I in the ADRY agent-induced cyclic electron flow can be answered by the investigation of the 703-nm absorption change. The amplitude of the 703-nm reduction kinetics in short flashes (20 μs) represents the number of electrons flowing through System I[18,19]. Because of the functional coupling between different chlorophyll a_I centers[19] and of the high equilibrium constants between chlorophyll a_I and the primary electron donors[19,20], practically all electrons (>90%) are transferred to chlorophyll a_I. If a cyclic electron flow around System I is prevented by the addition of an acceptor and in the absence of artificial System I electron donors, the above-mentioned 703-nm amplitude can be used as a measure for the electrons produced by System II. This has been clearly shown by comparitive studies of the 703-nm amplitude and the oxygen evolution as a function of the 3-(3,4-dichlorophenyl)-1,1-dimethylurea (DCMU) concentration under repetitive short-flash excitation conditions[21]. Therefore, a parallel decrease of the average oxygen yield per flash $\varphi(t_d)$ and of the 703-nm absorption change with increasing times t_d between the flashes would be expected, if the ANT 2s-induced cycle includes only Photosystem II (way B in Fig. 1). If on the other hand both light reactions participated in the ANT 2s-catalyzed cyclic flow (way C) the 703-nm am-

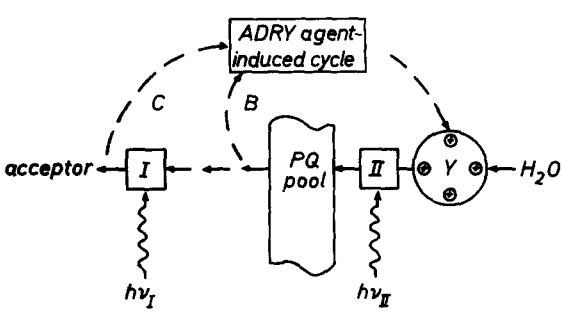

Fig. 1. Simplified scheme of possible ADRY agent-induced cyclic electron transport pathways. Symbols I and II refer to the centers of the light reactions I and II, respectively. Y, water-splitting enzyme system; PQ, plastoquinone. Symbol B characterizes an ADRY agent-induced cycle including only light reaction II, symbol C indicates a cycle including both light reactions.

plitude should remain constant with increasing times t_d, whereas the average oxygen yield per flash $\varphi(t_d)$ would decrease. But, because of the possibility that ANT 2s could also induce a separate cycle around System I, an amplitude of the 703-nm absorption change remaining constant with increasing t_d is not an unequivocal proof for the participation of both light reactions in the ANT 2s-induced cycle leading to the discharge of the higher-trapped-hole accumulation states. Hence, it is necessary to take into account a possible System I cycle, catalyzed by ANT 2s.

In Fig. 2 the relative average oxygen yield per flash $\varphi(t_d)$, as a function of the time t_d between the flashes, is compared with the corresponding amplitude of the

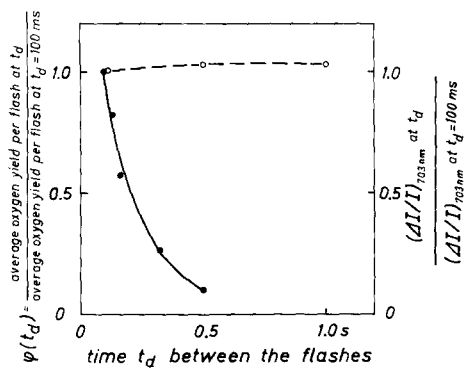

Fig. 2. Relative average oxygen yield per flash, $\varphi(t_d)$, and relative amplitude of the 703-nm absorption change as a function of the time t_d between the flashes. Experimental conditions as described in Materials and Methods. ○---○, $(\Delta I/I)_{703\,nm}$ at $t_d/(\Delta I/I)_{703\,nm}$ at $t_d = 100$ ms; ●—●, $\varphi(t_d)$.

703-nm absorption change in the presence of 10^{-6} M ANT 2s. It is clearly seen, that the amplitude remains constant in a time range, in which $\varphi(t_d)$ drastically decreases. If however, in addition, DCMU is present at a concentration ($2 \cdot 10^{-6}$ M) leading to the complete blockage of the electron transport from System II, the amplitude of the 703-nm absorption change is drastically decreased, so that an ANT 2s-induced separate cycle around System I can be excluded as an explanation for the 703-nm amplitude remaining constant with increasing time t_d. Hence, from the experimental data of Fig. 2 it can be inferred that ANT 2s catalyzes the discharge of S_2 and S_3 by a cycle including both light reactions.

Now it remains to be shown whether the action of Photosystem I is a prerequisite for the ADRY effect induced by ANT 2s. To clarify this question a selective inhibition of System I (without affecting System II) is required. Recently it has been found, that 2,5-dibromo-3-methyl-6-isopropyl-1,4-benzoquinone (DBMIB) blocks the electron transport chain at the plastoquinone pool[22] and that histone inhibits in the neighborhood of Photosystem I[23].

In the following experiments a histone treatment (as described in ref. 23) was used which causes a significant decrease of the 703-nm amplitude without a remarkable influence on the oxygen evolution in the presence of $K_3[Fe(CN)_6]$ as electron acceptor.

In respect to the DBMIB effect it has been found that this agent drastically decreases the rate of the electron flow from System II to P700 without influence on

the oxygen evolution. In Fig. 3 the average oxygen yield per flash as a function of the time t_d between the flashes in the presence of $3 \cdot 10^{-7}$ M ANT 2s is given for normal and for histone-treated chloroplasts. Although a slight difference between both curves can be observed, the results clearly show, that ANT 2s exerts an ADRY effect in histone-treated chloroplasts, too. Similar results were obtained for DBMIB-blocked chloroplasts (see Fig. 3). Hence, the conclusion can be drawn, that for the ADRY effect of ANT 2s the functioning of System I is not required. In this way either pathway B or C can be realized, depending on the experimental conditions. These results show, that a functional specific electron donor is not required for the discharge of the trapped holes catalyzed by the ADRY agents.

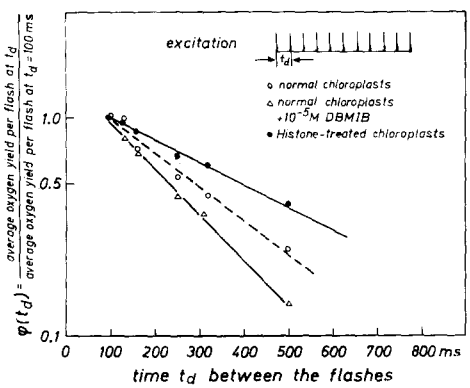

Fig. 3. Relative average oxygen yield per flash, $\varphi(t_d)$, as a function of the time t_d between the flashes under different conditions of System I activity. Histone treatment or DBMIB addition as indicated in the figure. Other experimental conditions as described in Materials and Methods. Ordinate: logarithmic.

The mechanism of the ANT 2s-induced cyclic electron flow

(A) Characterisation of different models

For the mechanism of the ADRY agent-catalyzed discharge of the higher-trapped-hole accumulation states generally two possibilities have to be distinguished: (i) A fixed-place mechanism whereby the catalyst is assumed to be strongly bound at specific sites within the water-splitting enzyme system Y, thereby changing the trapped-hole discharge rate. That means: the lingering time of ANT 2s at the binding sites is long so that during the course of one illumination period (maximal 120 s, see ref. 10) no exchange of ANT 2s between the free and the occupied sites of different Y systems takes place. (ii) A mobile-catalyst mechanism. In this mechanism the ANT 2s catalyst is diffusible between different water-splitting enzyme systems Y.

A distinction between both mechanisms is possible on the basis of the fundamental results obtained by Joliot *et al.*[1] and by Forbush *et al.*[2]. According to their experiments it has been unequivocally proved, that the watersplitting enzyme systems Y act as functional independent units, *i.e.* no trapped-hole cooperation occurs between different Y systems. Hence, the Y systems are independent units also in respect to the discharge reactions of S_2 and S_3. Firstly the fixed-place mechanism is discussed.

Each water splitting enzyme system Y is assumed to have n binding sites for ANT 2s. Therefore, $n+1$ different ANT 2s-labeled states of Y, each characterized by

its own decrease function $\varphi_m(t_d)$ for the average oxygen yield per flash (with $m=0,1,\ldots n$), can be distinguished. Furthermore, equal affinities for ANT 2s will be assumed for all sites, *i.e.* cooperative binding effects[24] will be excluded. Under these conditions

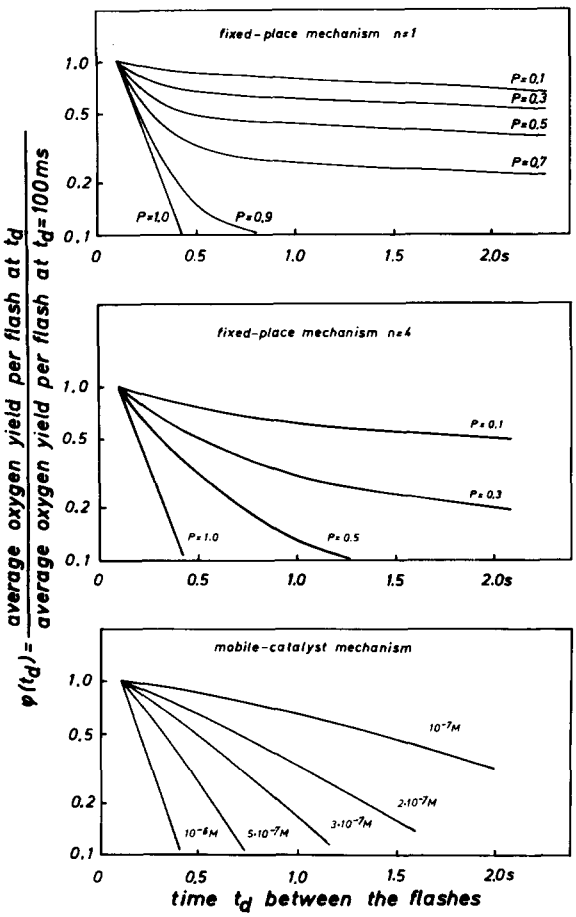

Fig. 4. Theoretical curves of the relative average oxygen yield per flash, $\varphi(t_d)$, as a function of the time t_d between the flashes computed for different models. Ordinate: logarithmic.

Top: Fixed-place mechanism with one binding site for ANT 2s per system Y, $\varphi(t_d)$ computed according to Eqn 2. Assumptions:

$$\varphi_{\text{normal}}(t_d)=e^{-k_{\text{normal}}(t_d-0.1\text{ s})},\quad k_{\text{normal}}=0.14\text{ s}^{-1}$$

$$\varphi_{\text{ANT 2s}}(t_d)=e^{-k_{\text{ANT 2s}}(t_d-0.1\text{ s})},\quad k_{\text{ANT 2s}}=6.9\text{ s}^{-1}$$

Middle: Fixed-place mechanism with four binding sites for ANT 2s per system Y, $\varphi(t_d)$ computed according to Eqn 1. Assumptions:

$$\varphi_m(t_d)=e^{-k_m(t_d-0.1\text{ s})}$$

with $k_0=0.14\text{ s}^{-1}$; $k_1=1.7\text{ s}^{-1}$; $k_2=3.45\text{ s}^{-1}$; $k_3=5.2\text{ s}^{-1}$; $k_4=6.9\text{ s}^{-1}$.

Bottom: Mobile-catalyst mechanism, evaluation according to Eqns 9 and 10. Assumptions: $\alpha=0.2$; $k=0.46\text{ s}^{-1}$ for $c_{\text{ANT 2s}}=10^{-7}$ M; $k=0.92\text{ s}^{-1}$ for $c_{\text{ANT 2s}}=2.10^{-7}$ M; $k=1.39\text{ s}^{-1}$ for $_{\text{ANT 2s}}=3\cdot10^{-7}$ M; $k=2.31\text{ s}^{-1}$ for $c_{\text{ANT 2s}}=5\cdot10^{-7}$ M and $k=4.62\text{ s}^{-1}$ for $c_{\text{ANT 2s}}=10^{-7}$ M.

the relative average oxygen yield per flash $\varphi(t_d)$ of the whole ensemble is given by:

$$\varphi(t_d) = \sum_{m=0}^{n} \binom{n}{m} P^m (1-P)^{n-m} \cdot \varphi_m(t_d) \tag{1}$$

where P is the mean probability, that a binding site is occupied. The mean probability is related to the ANT 2s concentration by the partition coefficients and the binding constant. P is proportional to the total concentration of ANT 2s. If only one binding site per Y system was present ($n=1$), then $\varphi(t_d)$ is the sum of only two terms (Eqn 2):

$$\varphi(t_d) = P \cdot [\varphi(t_d)]_{\text{ANT 2s}} + (1-P) \cdot [\varphi(t_d)]_{\text{normal}} \tag{2}$$

Therefore, a two-phase kinetic pattern should be observed with a linear dependence of the amplitude P on the ANT 2s concentration. Since $[\varphi(t_d)]_{\text{ANT 2s}}$ is distinguished from $[\varphi(t_d)]_{\text{normal}}$ by more than one order of magnitude[10], a clear separation of the two kinetics should be observable, as is seen in Fig. 4 (top) for the case of $[\varphi(t_d)]_{\text{normal}}$ and $[\varphi(t_d)]_{\text{ANT 2s}}$ being first-order decay curves.

The situation is even more complicated if more than one binding site is present per Y system. In this case a different kinetic pattern arises. This is shown in Fig. 4 (middle) for $n=4$, where again in a first-order approximation the curves $\varphi_m(t_d)$ with $m=0,\ldots 4$ are assumed to be exponential with rate constants k_m being linearly related to the number m of ANT 2s bound per Y system. In this case the resulting curves for $\varphi(t_d)$ only slightly deviate from a first-order decay. Contrary to the fixed-place mechanism in the mobile-catalyst mechanism it is supposed, that ANT 2s diffuses to the higher-trapped-hole accumulation states building up a temporary complex, thereby modifying the stability of the stored holes. Two consecutive steps take place (see ref. 25):

$$\oplus_{\text{trap}} + \text{ANT 2s} \underset{k_{-1}}{\overset{k_1}{\rightleftharpoons}} [\oplus_{\text{trap}} \ldots \text{ANT 2s}] \tag{3}$$

$$[\oplus_{\text{trap}} \ldots \text{ANT 2s}] + e \xrightarrow{k_2} \circ_{\text{trap}} + \text{ANT 2s} \tag{4}$$

In the mobile-catalyst mechanism the lingering time of ANT 2s at the binding site corresponds with the life-time of the complex $[\oplus_{\text{trap}} \ldots \text{ANT 2s}]$.

Two cases will be considered:

(a) $k_1, k_{-1} \gg k_2$, *i.e.* equilibration between $\oplus_{\text{trap}}$ and ANT 2s occurs.

The decay kinetics of a higher-trapped-hole accumulation state symbolized by $\oplus_{\text{trap}}$ is given by:

$$-\frac{d[\oplus_{\text{trap}}]}{dt} = k_2 \cdot \frac{k_1}{k_{-1}} [\text{ANT 2s}] \cdot [\oplus_{\text{trap}}] \cdot [e] \tag{5}$$

(b) $k_2 \cdot [e] \gg k_1$, *i.e.* the complex concentration $[\oplus_{\text{trap}} \ldots \text{ANT 2s}]$ is very low.

Now the decay kinetics are described by:

$$-\frac{d[\oplus_{\text{trap}}]}{dt} = k_1 [\text{ANT 2s}] \cdot [\oplus_{\text{trap}}] \tag{6}$$

It is seen, that in both cases the deactivation rate of the higher-trapped-hole accumulation states depends linearly on the ANT 2s concentration.

However, the experimentally determined relative average oxygen yield per flash $\varphi(t_d)$ as a function of the time t_d between the flashes, depends on the discharge rates of the two higher-trapped-hole accumulation states S_2 and S_3, respectively. Therefore, the function $\varphi(t_d)=$f(ANT 2s concn) is expected to be complex even for the simplest case, in which the discharge rates of S_2 and S_3 are first-order kinetics.

According to the model of Forbush *et al.*[2], the oxygen yield of a short flash is determined by the number of water-splitting enzyme systems being in the trapped-hole accumulation state S_3 just before the excitation with the flash. Hence, the relative average oxygen yield per flash is given by:

$$\varphi(t_d)=N_0\cdot[S_3(t_d)] \tag{7}$$

N_0 is the normalization constant given as the reciprocal value of the average oxygen yield per flash at $t_d=100$ ms (see ref. 10). Under steady-state conditions including a one-step deactivation mechanism, the relative average oxygen yield per flash $\varphi(t_d)$ can be evaluated by Eqn 8 (see Appendix):

$$\varphi(t_d)=N_0\cdot\frac{\det A}{\det B} \tag{8}$$

The determinants det A and det B are given explicitly in the Appendix. By introduction of suitable approximations (see Appendix) one obtains:

$$\varphi(t_d)=\frac{N_0(1-\alpha)^2\cdot e^{-2kt_d}}{(2-5\alpha+4\alpha^2)\cdot e^{-2kt_d}+(1-3\alpha)\cdot e^{-kt_d}+1} \tag{9}$$

where α is the probability of "misses" (see ref. 2) and k, the rate constant for the assumed first-order one-step deactivation of S_2 and S_3, respectively.

In Fig. 4 (bottom) a few examples for $\varphi(t_d)$ evaluated according to Eqn 9 are shown, taking into account the linear relationship between the rate constants k and the ANT 2s concentration. As a reference the rate constant k (10^{-6} M) obtained as a most suitable fit for the decay curve at 10^{-6} M ANT 2s is used. Then the other rate constant can be evaluated according to Eqn 10:

$$k(c_{\text{ANT 2s}})=k(10^{-6}\text{ M})\cdot\frac{c_{\text{ANT 2s}}}{10^{-6}} \tag{10}$$

It is seen, that the curves $\varphi(t_d)$ are not first-order decay kinetics. Contrary to the convex deviation from a first-order decay of the experimental data (see refs 9, 10 and 12), the curves given by Eqn 9 show a concave deviation from the first-order plot. Hence, the approximations involved in Eqn 9 are excessive, but for a more qualitative discussion the correspondence between the experimental data and the theoretical curves is sufficient.

(B) The decay of the dependence of the relative average oxygen yield per flash on the ANT 2s concentration. Comparison with the proposed models (fixed place or mobile catalyst)

In Fig. 5 the time course of $\varphi(t_d)$ is given for different concentrations of ANT

2s. At ANT 2s concentrations higher than 10^{-6} M only a slight increase of the deactivation rate is observed with a concomitant strong inhibitory effect on the water-splitting enzyme system Y. On the other hand, at ANT 2s concentrations lower than 10^{-7} M, the differences between the decay curves of $\varphi(t_d)$ induced by ANT 2s and the decay of $\varphi(t_d)$ caused by the natural deactivation processes, reach the limit of the sensitivity of the polarographic measuring device.

Therefore, in the present paper only the concentration range of 10^{-7}–10^{-6} M ANT 2s will be considered. Furthermore, it is assumed, that at 10^{-6} M ANT 2s the maximal decay rate of $\varphi(t_d)$ is practically reached (at higher concentration only a slight increase of the decay rate is observed), irrespective of the mechanism (fixed place or mobile catalyst) of the ADRY effect. Hence, a concentration of 10^{-6} M ANT 2s in the mobile-catalyst mechanism corresponds with a mean occupancy probability of 1 in the fixed-place mechanism. This point will be used as the reference for the comparison of both mechanisms.

If one takes into account that the mean occupancy probability P is linearly related to the total ANT 2s concentration, a direct comparison is possible.

On the basis of these considerations, a fixed-place mechanism with only one binding site for ANT 2s per system Y ($n=1$) can be excluded because of the significant differences between the curves of Fig. 4 (top) and Fig. 5. The same clear distinction is not observed by comparison of the experimental results of Fig. 5 with a fixed-place mechanism including four binding sites (Fig. 4, middle) and the mobile-catalyst mechanism (Fig. 4, bottom).

However, qualitative conclusions can be drawn on the basis of the dependence of the decay rates of $\varphi(t_d)$ on the ANT 2s concentrations. Taking into account the linear relationship between the ANT 2s concentration and the mean occupancy

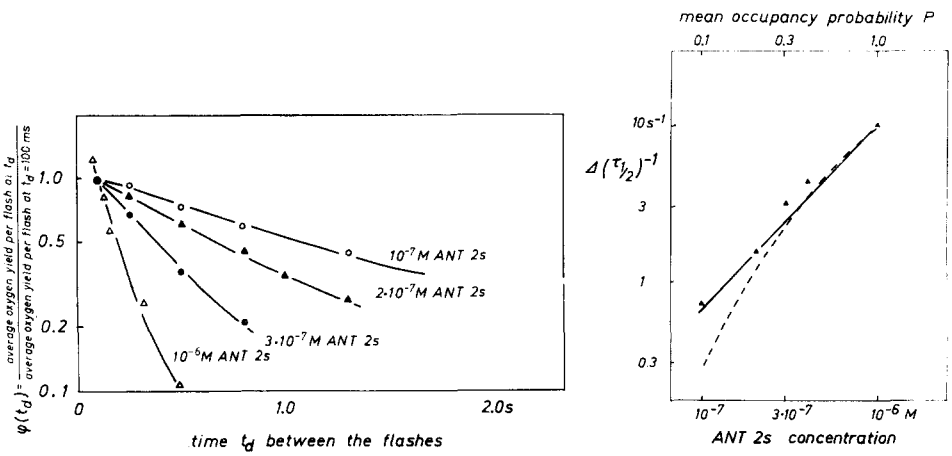

Fig. 5. Relative average oxygen yield per flash, $\varphi(t_d)$, as a function of the time t_d between the flashes at different ANT 2s concentrations. ANT 2s concentration as indicated in the figure. Other experimental conditions as described in Materials and Methods. Ordinate: logarithmic.

Fig. 6. ANT 2s-induced reciprocal half time increment of the decay of the relative average oxygen yield per flash $\Delta(\tau_{1/2})^{-1}$ as a function of the ANT 2s concentration. The curves are calculated from the theoretical curves presented in Fig. 4 (middle) and Fig. 4 (bottom) according to Eqn 11 with $(\tau_{1/2})_{normal}=0.2\ s^{-1}$. – – – –, curve for the fixed-place mechanism with $n=4$; ———, curve for the mobile-catalyst mechanism; full triangles are experimental values $\Delta(\tau_1)^{-1}$ derived from Fig. 5.

probability P a direct comparison is possible with the experimental data. As a measure of the decay rate of $\varphi(t_d)$ the reciprocal half time $(\tau_{1/2})_{ANT2s}$ will be used. In order to eliminate the decay caused by the natural deactivation processes, the reciprocal half time of the normal decay $(\tau_{1/2})^{-1}_{normal}$ (0.2 s^{-1}) will be substracted:

$$\Delta(\tau_{\frac{1}{2}})^{-1} = (\tau_{\frac{1}{2}})^{-1}_{ANT\ 2s} - (\tau_{\frac{1}{2}})^{-1}_{normal} \tag{11}$$

In Fig. 6 the ANT 2s induced increment $\Delta(\tau_{1/2})^{-1}$ of the reciprocal half time as a function of the ANT 2s concentration, is compared with the theoretical curves evaluated from Fig. 4, middle and bottom, respectively. It is seen that the experimental data are in closer correspondence with a mobile-catalyst mechanism.

Hence, the conclusion can be drawn, that the ADRY effect is probably caused by a mobile-catalyst mechanism. But, keeping in mind all the approximations (included in Fig. 4) leading to the theoretical curves of Fig. 6, the above conclusion is valid only qualitatively.

Summarizing the results, it is shown in the present paper for the example of ANT 2s, that no special endogenous electron donor is required for the ADRY agent-catalyzed discharge of the higher-trapped-hole accumulation states. Furthermore, the System I activity is not a functional indispensable element of the ADRY agent-induced cyclic electron flow. The ADRY agents probably act as mobile catalysts rather than in a fixed-place mechanism.

APPENDIX

According to the four-step model of Forbush *et al.*[2] the processes of the oxygen evolution can be described by the scheme:

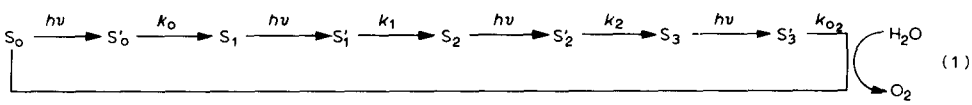

(1)

In the dark the states S_2 and S_3 are discharged by one-step and two-step deactivation processes (see ref. 1):

$$S_3 \overset{k_{-3}}{\rightarrow} S_2 \overset{k_{-2}}{\rightarrow} S_1 \tag{2a}$$

One step deactivation

$$S_2 \overset{k_{-2}}{\rightarrow} S_1 \tag{2b}$$

$$S_3 \overset{k'_{-3}}{\rightarrow} S_1 \tag{3a}$$

Two-step deactivation

$$S_2 \overset{k'_{-2}}{\rightarrow} S_0 \tag{3b}$$

By excitation with short saturating flashes (approx. 20 μs) and at times t_d between the flashes which are long in comparison to the dark reaction times of the states S'_i, each flash induces practically one turnover in System II. Because of the flash tails (see refs 1 and 2) a double hit probability β exists. Furthermore, the system includes a probability factor of "misses" α_1 describing the percentage of centers which are not

converted by the flash (see ref. 2). Taking into account these factors and firstly neglecting the deactivation processes, the distribution of the states $S_0, \ldots S_3$ after the $(n+1)$th flash of a flash sequence is given by:

$$[S_0]_{n+1} = (1-\alpha_3 - \beta)\ S_3]_n + \beta[S_2]_n + \alpha_0[S_0]_n \tag{4a}$$

$$[S_1]_{n+1} = (1-\alpha_0-\beta)[S_0]_n + \beta[S_3]_n + \alpha_1[S_1]_n \tag{4b}$$

$$[S_2]_{n+1} = (1-\alpha_1-\beta)[S_1]_n + \beta[S_0]_n + \alpha_2[S_2]_n \tag{4c}$$

$$[S_3]_{n+1} = (1-\alpha_2-\beta)[S_2]_n + \beta[S_1]_n + \alpha_3[S_3]_n \tag{4d}$$

$[S_i]$ = probability, that a water-splitting enzyme system Y is in the activation state S_i $(i=0, \ldots 3)$; n and $n+1$ refer to the distributions of S_i after the nth and the $(n+1)$th flash, respectively.

For the following considerations of the trapped-hole discharge reactions only the one-step deactivation processes (2a, 2b) will be included.

If the dark time between the equidistant flashes is t_d, then for all flashes the relationships

$$[S_3(t_d)] = [S_3(0)]\delta_3(t_d) \tag{5a}$$

$$[S_2(t_d)] = [S_2(0)]\delta_2(t_d) + [S_3(0)]\delta_{32}(t_d) \tag{5b}$$

hold, where $\delta_2(t_d)$ and $\delta_3(t_d)$ are defined as "deactivation functions" representing the the fraction of S_2 and S_3 remaining after the time t_d in the activation state S_i $(i=2$ or 3) produced by the flash. According to Eqn 2a S_2 is also formed as an intermediate in the deactivation of S_3. For this process a new "deactivation function" $\delta_{32}(t_d)$ is introduced giving that part of S_2 which is built up from $S_3(0)$.

By introduction of Eqns 5a and 5b into 4a–4d one obtains:

$$[S_0(t_d)]_{n+1} = (1-\alpha_3-\beta)[S_3(t_d)]_n + \beta[S_2(t_d)]_n + \alpha_0[S_0(t_d)]_n \tag{6a}$$

$$\begin{aligned}[S_1(t_d)]_{n+1} = {} & \alpha_1[S_1(t_d)]_n + \beta[S_3(t_d)]_n + (1-\alpha_0-\beta)[S_0(t_d)]_n \\ & + \{(1-\alpha_1-\beta)[S_1(t_d)]_n + \beta[S_0(t_d)]_n + \alpha_2[S_2(t_d)]_n\}\{1-\delta_2(t_d)\} \\ & + \{(1-\alpha_2-\beta)[S_2(t_d)]_n + \beta[S_1(t_d)]_n + \alpha_3[S_3(t_d)]_n\}\{1-\delta_{32}(t_d)-\delta_3(t_d)\}\end{aligned} \tag{6b}$$

$$\begin{aligned}[S_2(t_d)]_{n+1} = {} & \{(1-\alpha_1-\beta)[S_1(t_d)]_n + \beta[S_0(t_d)]_n + \alpha_2[S_2(t_d)]_n\}\delta_2(t_d) \\ & + \{(1-\alpha_2-\beta)[S_2(t_d)]_n + \beta[S_1(t_d)]_n + \alpha_3[S_3(t_d)]]\}\delta_{32}(t_d)\end{aligned} \tag{6c}$$

$$[S_3(t_d)]_{n+1} = \{(1-\alpha_2-\beta)[S_2(t_d)]_n + \beta[S_1(t_d)]_n + \alpha_3[S_3(t_d)]_n\}\delta_3(t_d) \tag{6d}$$

Under steady state the relationship

$$[S_i(t_d)]_{n+1} = [S_i(t_d)]_n \tag{7}$$

is valid for all states $(i=0, \ldots 3)$ and flashes.

With this steady-state condition and by introduction of the conservation condition $\sum_{i=0}^{3} S_i = 1$, one obtains from 6a–6d the nonhomogeneous equation system 8a–8d for the steady-state distribution of the states S_i (subscripts n are omitted):

$$(1-\alpha_0)[S_0(t_d)]-\beta[S_2(t_d)]-(1-\alpha_3-\beta)[S_3(t_d)]=0 \tag{8a}$$

$$\beta\delta_2(t_d)[S_0(t_d)]+\{(1-\alpha_1-\beta)\delta_2(t_d)+\beta\delta_{32}(t_d)\}[S_1(t_d)] + \{(1-\alpha_2-\beta)\delta_{32}(t_d)-1-\alpha_2\delta_2 1(t_d)]\}[S_2(t_d)]+\alpha_3\delta_{32}(t_d)[S_3(t_d)]=0 \tag{8b}$$

$$\beta\delta_3(t_d)[S_1(t_d)]+(1-\alpha_2-\beta)\delta_3(t_d)[S_2(t_d)]-\{1-\alpha_3\delta_3(t_d)\}[S_3(t_d)]=0 \tag{8c}$$

$$[S_0(t_d)]+[S_1(t_d)]+[S_2(t_d)]+[S_3(t_d)]=1 \tag{8d}$$

From this system the steady-state probability of the state S_3 as a function of the time t_d can be evaluated by:

$$S_3(t_d)=\frac{\det A}{\det B} \tag{9}$$

with

$$\det A=\begin{vmatrix} 1-\alpha_0 & 0 & -\beta \\ \beta\delta_2(t_d) & (1-\alpha_1-\beta)\delta_2(t_d)+\beta\delta_{32}(t_d) & (1-\alpha_2-\beta)\delta_{32}(t_d)-[1-\alpha_2\delta_2(t_d)] \\ 0 & \beta\delta_3(t_d) & (1-\alpha_2-\beta)\delta_3(t_d) \end{vmatrix}$$

$$\det B=\begin{vmatrix} 1-\alpha_0 & 0 & -\beta & -(1-\alpha_3-\beta) \\ \beta\delta_2(t_d) & (1-\alpha_1-\beta)\delta_2(t_d)+\beta\delta_{32}(t_d) & (1-\alpha_2-\beta)\delta_{32}(t_d)-[1-\alpha_2\delta_2(t_d)] & \alpha_3\delta_{32}(t_d) \\ 0 & \beta\delta_3(t_d) & (1-\alpha_2-\beta)\delta_3(t_d) & -[1-\alpha_3\delta_3(t_d)] \\ 1 & 1 & 1 & 1 \end{vmatrix}$$

Hence, the relative average oxygen yield per flash is given by:

$$\varphi(t_d)=N_0\frac{\det A}{\det B} \tag{10}$$

The evaluation of Eqn 9 gives a complicated explicit formula for $\varphi(t_d)$. However, by introduction of suitable approximations a simple algebraic form can be obtained.

These approximations include: α_i is assumed to be equal for all states ($\alpha_i=\alpha$ for $i=0,\ldots 3$) $\beta\sim 0$ (see ref. 4); as was shown in ref. 14 $\delta_2(t_d)\sim\delta_3(t_d)\sim\exp(-kt_d)$ can be used as a reasonable approximation; furthermore, the influence of $\delta_{32}(t_d)$ is small and will be neglected. Then one obtains:

$$\varphi(t_d)=\frac{N_0(1-\alpha)^2\cdot e^{-2kt_d}}{(2-5\alpha+4\alpha^2)\cdot e^{-2kt_d}+(1-3\alpha)\cdot e^{-kt_d}+1} \tag{10}$$

ACKNOWLEDGEMENTS

The author is very grateful to Dr Ch. Wolff for very fruitful discussions and a critical reading of the manuscript. He wishes to thank Dr K. H. Buchel, Bayer Forschungszentrum, Wuppertal-Elberfeld, for the gift of the 2-anilinothiophenes and Professor Dr A. Trebst for the gift of DBMIB.

The skillful technical assistance of Miss S. Veit is gratefully acknowledged.

REFERENCES

1 Joliot, P., Joliot, A., Bouges, B. and Barbieri, G. (1971) *Photochem. Photobiol.* 14, 287–305
2 Forbush, B., Kok, B. and McGloin, M. P. (1971) *Photochem. Photobiol.* 14, 307–321
3 Vater, J., Renger, G., Stiehl, H. H. and Witt, H. T. (1969) in *Progress in Photosynthesis Research Freudenstadt, 1968* (Metzner, H., ed.), Vol. 2, pp. 1006–1008, H. Laupp Jr., Tübingen
4 Bouges-Bocquet, B. (1973) *Biochim. Biophys. Acta* 292, 772–785
5 De Kouchkovsky, Y. and Joliot, P. (1967) *Photochem. Photobiol.* 6, 567–587
6 Lemasson, C. (1970) *C. R. Acad. Sci. (Paris)* 270, 250–253
7 Lemasson, C and Barbieri, G. (1971) *Biochim. Biophys. Acta* 245, 386–397
8 Renger, G. (1969) *Naturwissenschaften* 56, 370
9 Renger, G. (1971) *Z. Naturforsch.* 26b, 149–153
10 Renger, G. (1972) *Biochim. Biophys. Acta* 256, 428–439
11 Renger, G., Bouges-Bocquet, B. and Büchel, K. H. (1973) *J. Bioenerg.* 4, 491–505
12 Renger, G. (1972) *Eur. J. Biochem.* 27, 259–269
13 Vater, J. (1973) *Biochim. Biophys. Acta* 292, 786–795
14 Renger, G., Bouges, B. and Delosme, R. (1973) *Biochim. Biophys. Acta* 292, 796–807
15 Winget, G. D., Izawa, S. and Good, N. E. (19—) *Biophys. Biochem. Res. Commun.* 21, 438–443
16 Vater, J. (1971), Thesis, Technical University Berlin
17 Döring, G., Stiehl, H. H. and Witt, H. T. (1967), *Z. Naturforsch.* 22b, 639–644
18 Rumberg, B. (1964) *Z. Naturforsch.* 19b, 707–716
19 Haehnel, W. (1973) *Biochim. Biophys. Acta* 305, 618–631
20 Marsho, T. V. and Kok, B. (1970) *Biochim. Biophys. Acta* 223, 240–250
21 Siggel, U., Renger, G. and Rumberg, B. (1972) in *Proc. 2nd Int. Congr. Photosynthesis Res., Stresa, 1971* (Forti, G., Avron, M. and Melandri, A., eds), Vol. 1, pp. 753–762, Dr. W. Junk N. V. Publishers, The Hague
22 Trebst, A., Harth, E. and Draber, W. (1970) *Z. Naturforsch.* 25b, 1157–1159
23 Brand, I., Baszynski, T., Crane, F. L. and Krogmann, D. W. (1972) *J. Biol. Chem.* 247, 2814–2819
24 Monod, J., Wyman, J. and Changeux, J. P. (1965) *J. Mol. Biol.* 12, 88–118
25 Renger, G. (1972) *Physiol. Vég.* 10, 239–345